JOURNAL OF NATURAL PRODUCTS

pubs.acs.org/jnp

Article

Metabolite and Molecular Characterization of *Mitragyna speciosa* Identifies Developmental and Genotypic Effects on Monoterpene Indole and Oxindole Alkaloid Composition

Larissa C. Laforest, Michelle A. Kuntz, Siva Rama Raju Kanumuri, Sushobhan Mukhopadhyay, Abhisheak Sharma, Sarah E. O'Connor, Christopher R. McCurdy, and Satya Swathi Nadakuduti*

Cite This: https://doi.org/10.1021/acs.jnatprod.3c00092

Read Online

ACCESS | Metrics & More | Article Recommendations | Supporting Information

ABSTRACT: The monoterpene indole alkaloid (MIA) mitragynine has garnered attention as a potential treatment for pain, opioid use disorder, and opioid withdrawal because of its combined pharmacology at opioid and adrenergic receptors in humans. This alkaloid is unique to *Mitragyna speciosa* (kratom), which accumulates over 50 MIAs and oxindole alkaloids in its leaves. Quantification of 10 targeted alkaloids from several tissue types and cultivars of *M. speciosa* revealed that mitragynine accumulation was highest in leaves, followed by stipules and stems, but was absent, along with other alkaloids, in roots. While mitragynine is the predominant alkaloid in mature leaves, juvenile leaves accumulate higher amounts of corynantheidine and speciociliatine. Interestingly, corynantheidine has an inverse relationship with mitragynine accumulation throughout leaf development. Characterization of various cultivars of *M. speciosa* indicated altered alkaloidal profiles ranging from undetectable to high levels of mitragynine. DNA barcoding and phylogenetic analysis using ribosomal *ITS* sequences revealed polymorphisms leading *M. speciosa* cultivars having lower mitragynine content to group with other mitragyna species, suggesting interspecific hybridization events. Root transcriptome analysis of low- and high-mitragynine-producing cultivars indicated significant differences in gene expression and revealed allelic variation, further supporting that hybridization events may have impacted the alkaloid profile of *M. speciosa*.

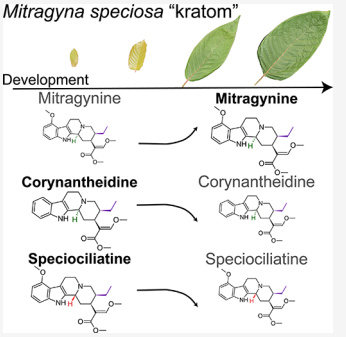

Mitragyna speciosa, also known as kratom, is a tree species belonging to the Rubiaceae (coffee family).[1] Kratom leaves have long been used ethnobotanically, either by chewing leaves or as a tea for pain relief, for combating fatigue, and to alleviate opioid withdrawal.[1,2] Kratom leaves produce over 50 monoterpene indole and oxindole alkaloids,[3] with the major monoterpene indole alkaloid (MIA) being mitragynine (Scheme 1). Mitragynine and its metabolite, 7-hydroxymitragynine (7-HMG), have been shown to be responsible for kratom's analgesic and opioid withdrawal-alleviating effects.[4,5] The U.S. is amid a devastating opioid crisis that has led to more than 500,000 deaths between 1999 and 2020.[6] Recently, kratom products have gained popularity in the U.S. and Europe as alternatives for pain medications and self-treatment of opioid addiction.[7,8] Mitragynine, specifically, shows promise to be developed as a treatment for pain, opioid use disorder, and opioid withdrawal.[9−11]

Mitragynine is a partial human μ-opioid receptor (hMOR) agonist with activity at several adrenergic receptors.[10] Importantly, mitragynine was shown to have limited abuse potential and reduced opioid intake in two independent preclinical animal studies.[11,12] On the other hand, its metabolite, 7-HMG (Scheme 1), was readily self-administered, increased animal intake of other opiates, and was found to be a much more potent hMOR agonist than mitragynine.[11,12] However, 7-HMG is a minor constituent of kratom alkaloids, and amounts detected in fresh kratom leaves are typically minor or below the lower limit of quantification in multiple analytical studies. Most studies focusing on the pharmacology and pharmacokinetics have been performed on these two alkaloids in animal models.[4,11,12] In addition to these, several other alkaloids produced in kratom have also been associated with varied pharmaceutical uses.[13] For example, the mitragynine diastereomers speciociliatine and mitraciliatine are partial hMOR agonists.[5,14] In addition, the MIAs speciogynine and paynantheine have serotonergic activity and pharmaceutical potential as stimulants,[5,14] and the oxindole mitraphylline has demonstrated potential in regulating the plasticity of human monocytes and attenuating inflammatory responses.[15,16] However, little is known about the genetic basis underlying the accumulation of MIAs and oxindole alkaloids and their diversification in *M. speciosa*.

Received: February 4, 2023

Scheme 1. Biosynthetic Precursors and Monoterpene Indole Alkaloids (MIAs) and Oxindole Alkaloids Found in *Mitragyna speciosa*[a]

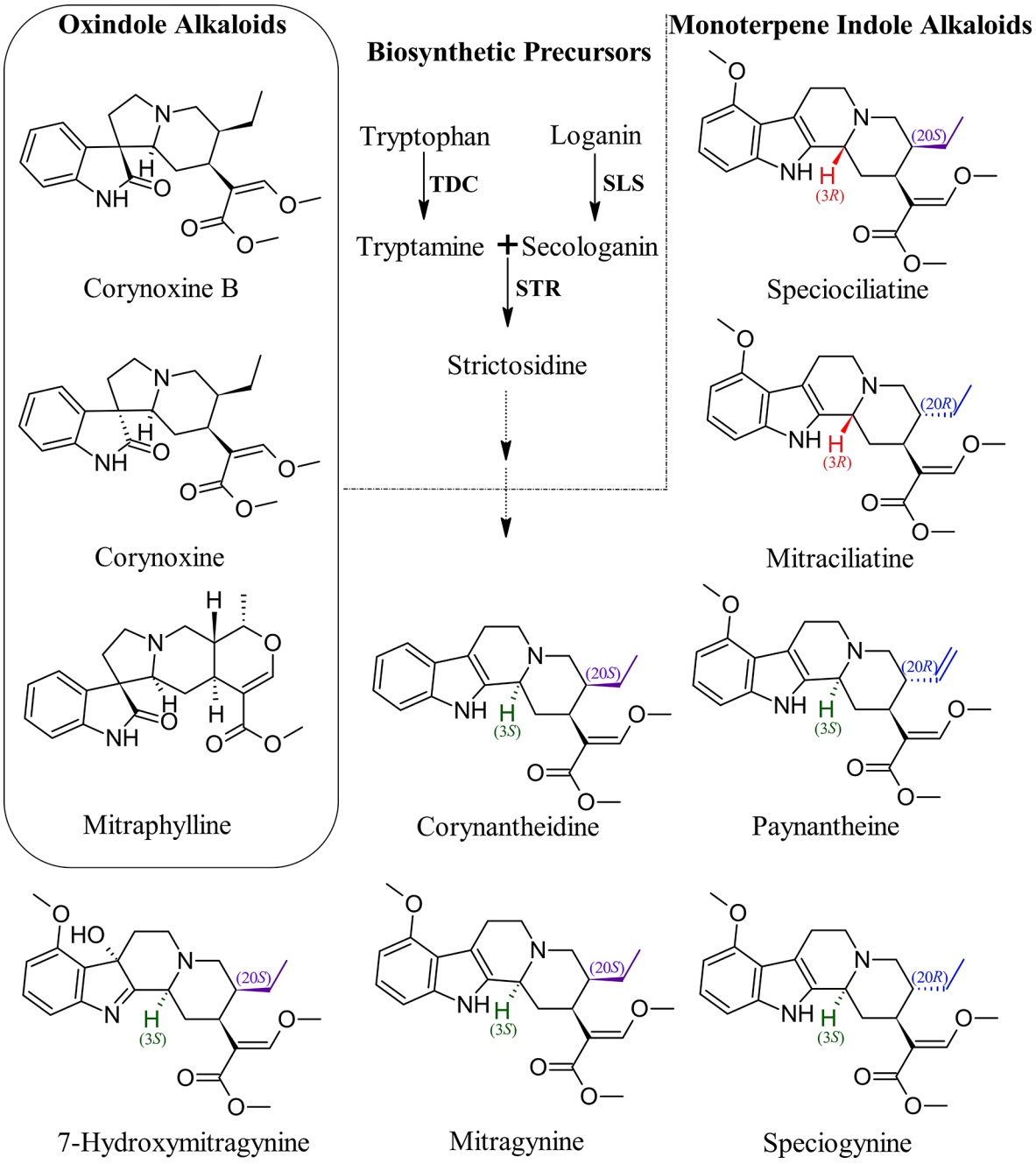

[a]Strictosidine formation is the first committed step toward MIA biosynthesis. Strictosidine is a product of the condensation of tryptophan-derived tryptamine and loganin-derived secologanin catalyzed by strictosidine synthase (STR). Strictosidine is the central intermediate for the downstream MIAs and oxindole alkaloids found in mitragyna, 10 of which are quantified in this study. TDC, tryptophan decarboxylase; SLS, secologanin synthase.

MIAs are one of the largest families of natural products, constituting important sources of medicinally significant compounds, often present at low concentrations within the species that produce them.[17] MIAs are highly diversified in structure and biological activities and are likely an evolutionary adaptation in plants against biotic and abiotic stresses. In addition, MIAs function in plant development and stimulus−response.[18] The range of chemical diversity in MIAs primarily originates from the central intermediate and common precursor strictosidine, formed by the condensation of the indoleamine tryptamine and the iridoid monoterpene secologanin catalyzed by strictosidine synthase (STR; *EC: 4.3.3.2*; Scheme 1).[17] One of the best-characterized MIA-producing species is *Catharanthus roseus*, mainly due to its production of the bisindole alkaloids vincristine and vinblastine, both of which are currently in use as chemotherapeutic drugs.[19,20]

M. speciosa is a tetraploid species ($2n = 4x = 44$) with a genome size of ∼1.45−1.56 Gb.[21,22] Comparative genomics investigating eight MIA-producing species, including *M.*

https://doi.org/10.1021/acs.jnatprod.3c00092
J. Nat. Prod. XXXX, XXX, XXX−XXX

speciosa, suggests that genomic loci involved in the MIA pathway are conserved.[18] Despite the pharmaceutical importance of mitragynine and other indole and oxindole alkaloids produced in *M. speciosa*, the downstream steps of MIA biosynthesis in this species are only recently being uncovered.[23] Other species of mitragyna, including *M. hirsuta*, *M. rotundifolia*, *M. diversifolia*, and *M. parvifolia*, are also used medicinally in various parts of the world to treat cough, hypertension, diarrhea, depression, fever, and pain.[1,24] These species accumulate either the oxindole alkaloid mitraphylline (Scheme 1) or the MIA mitraciliatine, but none produce mitragynine, which is unique to *M. speciosa*.[1,25] The various species of mitragyna have historically been identified by either floral or fruit morphology and further differentiated by DNA barcoding using the *nuclear ribosomal internal transcribed spacers* (*ITS*).[24] There is wide variation in alkaloidal profiles even among various *M. speciosa* cultivars, including cultivars with low mitragynine content in addition to accumulating mitraphylline, an MIA characteristic of other mitragyna species.[16,27] Furthermore, quantitative characterization of MIAs in whole plants and developmental variation of MIAs have not been studied comprehensively in *M. speciosa*.

In this study, whole-plant characterization of *M. speciosa* was performed by quantifying 10 pharmaceutically important MIAs and oxindole alkaloids (Scheme 1) from leaves of several developmental stages, stipules, stems, and roots. A mitragyna germplasm consisting of diverse *M. speciosa* cultivars and other mitragyna species was utilized to dissect their genetic and metabolite diversity by correlating their targeted alkaloid profiles with *ITS* DNA barcodes and phylogenetic analyses. Furthermore, root transcriptome profiling and analyses of MIA pathway homologues from no mitragynine and high mitragynine-producing cultivars were performed to reflect on the genetic basis of varying alkaloid profiles. Overall, this study lays a foundation for understanding the developmental variation of MIAs and oxindole alkaloids and diversification of stereochemistry in *M. speciosa* cultivars to inform the selection of new cultivars and its commercial cultivation.

RESULTS AND DISCUSSION

Characterization of Alkaloids from *M. speciosa* Identifies Differential Accumulation of Mitragynine and Other Alkaloids across Tissue Types and Developmental Stages. Targeted MIAs and oxindole alkaloids in Scheme 1 were quantified from *M. speciosa* leaves, stipules, stems, and roots. Overall, leaves accumulated the highest total alkaloids (1.73% w/w of dry weight), followed by stipules (1.13%). Stems (0.29%) and roots (0.20%) had minor or negligible amounts of alkaloids (Figure 1). Mitragynine was the predominant alkaloid in leaves, as expected. Notably, stipules, which are specialized leaf appendages that sheath developing leaves (Figure S1) also accumulated considerable amounts of mitragynine (Figure 1, Table S1) and could be economically useful apart from leaves. In contrast, stems had significantly less mitragynine, while it was undetectable in roots. Speciociliatine, a stereoisomer of mitragynine, was the most abundant alkaloid in stipules and stems, second only to mitragynine in leaves, and was also detected in roots. The high levels of mitragynine and speciociliatine found in stipules suggest a protective function for these alkaloids in plants against stresses until leaf emergence (Table S1).

Speciogynine and paynatheine were also detected in leaves and stipules. Interestingly, mitragynine and speciogynine

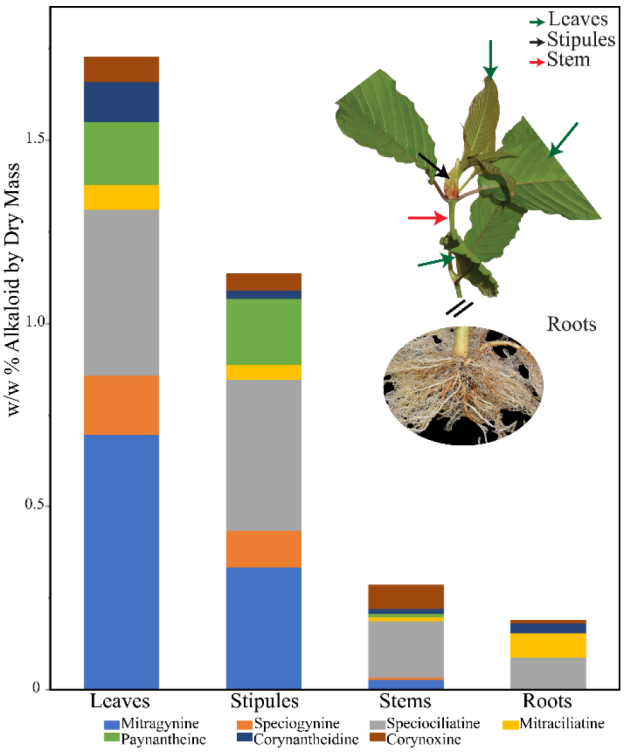

Figure 1. Characterization of alkaloids across tissue types in *M. speciosa*. (A) Stacked bar graph represents the relative quantification of alkaloids in varied tissue types of *M. speciosa* based on mean ($n = 3$) percentage weight by weight of dry tissue. Each color represents an individual alkaloid quantified. *M. speciosa* tissue types are denoted by arrows.

accumulation patterns trend together, and the ratio between them is maintained at ~3:1 in all tissues analyzed, including leaves, stipules, and stems (Figure 1, Table S1). Corynantheidine, the seemingly upstream precursor of mitragynine and speciogynine[23] (Scheme 1), was predominantly present in leaves (0.11%), and low levels were detected (<0.05%) in other tissues (Figure 1). While mitragynine, speciogynine, and paynantheine were detected in varying levels in all aerial tissue, none were detected in roots (Table S1). Rather, roots were characterized by low levels of speciociliatine, mitraciliatine, corynantheidine, and corynoxine (Figure 1). Thus, there appears to exist preferential accumulation of MIAs with 3*S* stereochemistry (Scheme 1) in aerial tissues regardless of the stereochemistry at the C-20 position, while 3*R* MIAs accumulate in all tissues (Table S1). This indicates a selective mechanism at play resulting in specific compartmental alkaloidal profiles. Levels of the minor oxindole alkaloid corynoxine were similar across aerial tissues but significantly lower in roots.

High variability was observed in leaf samples due to the pooled method of collection, comprising leaves of multiple developmental stages. RNA-seq evidence of *M. speciosa* tissues indicated that leaf expression of MIA genes is developmentally regulated.[21] For example, *STR* is highly expressed in juvenile leaves compared to mature leaves. Therefore, variability of targeted alkaloids across five leaf developmental stages defined as juvenile 1 (<4 cm; jv1), jv2 (<7 cm), jv3 (<10 cm), medium leaves (>10 cm), and mature leaves was quantitatively determined (Figure 2; Table 1). In juvenile tissues, corynantheidine and speciociliatine are the highest accumulat-

https://doi.org/10.1021/acs.jnatprod.3c00092
J. Nat. Prod. XXXX, XXX, XXX−XXX

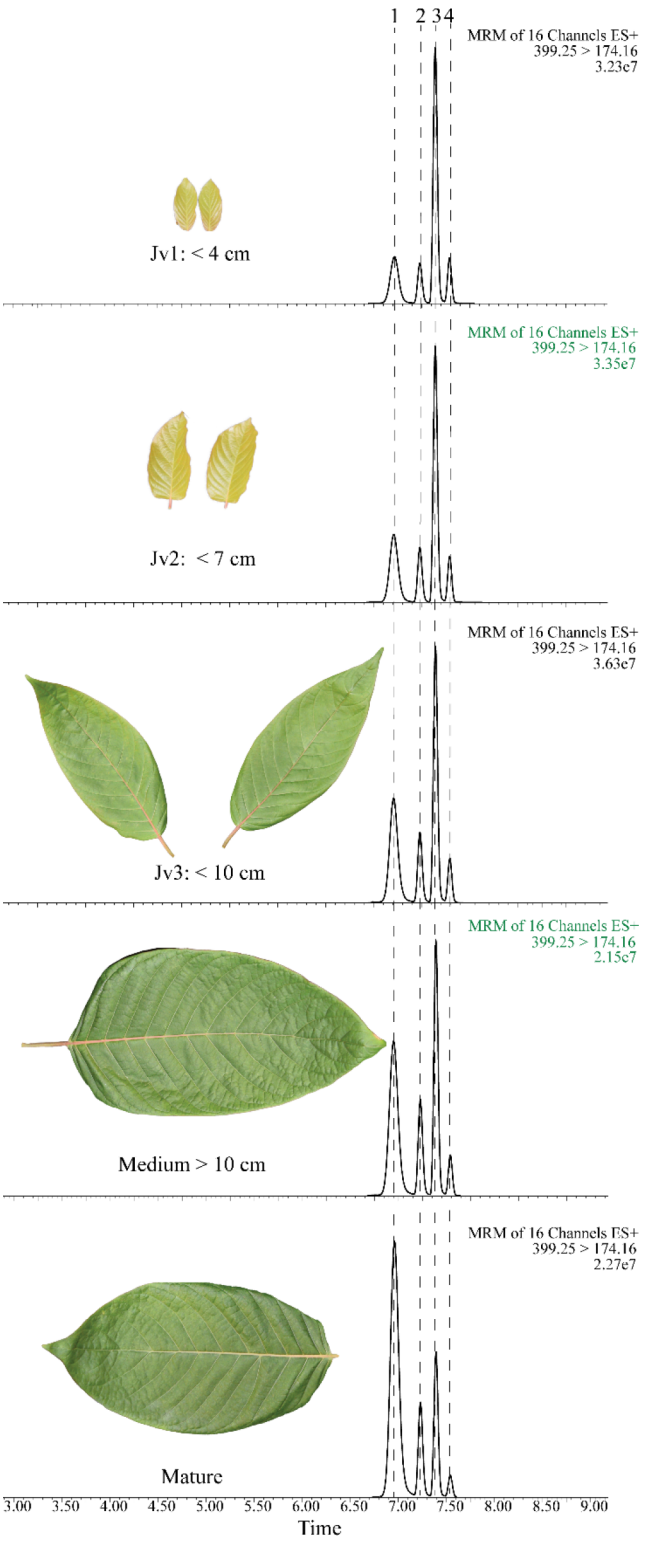

Figure 2. Developmental alkaloid profiling of leaves showing varying proportions of mitragynine and its stereoisomers. Three stages of juvenile leaves defined by jv1 < 4 cm, jv2 < 7 cm, and jv3 < 10 cm, medium leaves > 10 cm, and mature leaves were characterized for targeted alkaloids. Chromatograms of selected alkaloids (1) mitragynine, (2) speciogynine, (3) speciociliatine, and (4) mitraciliatine are identified and quantified based on their standards. Jv: juvenile.

ing alkaloids, unlike medium and mature leaves, where mitragynine dominates (Figure 2; Table 1). An inverse relationship between these compounds was observed as the leaf developed (R^2 0.488; Figure S2), with a steady decrease in corynantheidine and speciociliatine content and increased mitragynine, speciogynine, and paynantheine content. This negative correlation is in accordance with mitragynine formation occurring downstream of corynantheidine, as has recently been confirmed *in vitro*.[23] Notably, corynantheidine had an 18-fold reduction in content from juvenile leaves to mature leaves, with a 3-fold increase in mitragynine (Table 1). As observed across tissues, mitragynine and speciogynine content maintained similar accumulation patterns, with both increasing in leaf content across developmental stages (Figure 2). Further, the ratio between the C-20 epimers is maintained between 2:1 and 3:1 in all analyzed tissue (Table 1). On the other hand, the 3*R*-MIAs speciociliatine and mitraciliatine shared a similar downward trending accumulation pattern over leaf development. In this case, the ratio of speciociliatine (3*R*, 20*S*) to mitraciliatine (3*R*, 20*R*) is also maintained between 7:1 and 8:1. The opposite patterns of accumulation between 3*S* and 3*R* diastereomers indicate differences in the regulatory mechanisms governing their formation or accumulation, regardless of stereochemistry at the C-20 position.

Low to negligible levels (≤0.05% w/w) of 7-HMG were detected at all leaf developmental stages, while mitraphylline was not detected at any stage (Table 1). Mitragynine content increased by 2−3-fold in jv2 and jv3 compared to jv1 leaves. Similarly, speciogynine and paynantheine content also spiked significantly in jv2 and jv3 leaves. Taken together, this points to a rapid increase in the biosynthesis of 3*S* metabolism at early leaf developmental stages. The oxindole alkaloids corynoxine and corynoxine B however reduced in content as the leaf developed and matured. Overall, medium and mature leaves were characterized by an alkaloid profile predominantly represented by mitragynine and juvenile stages by corynantheidine. These drastic changes in alkaloid content between early developmental leaf stages and maturity are of high importance, as speciociliatine and corynantheidine may play a more major role in kratom pharmacology than expected but are often reported as minor *M. speciosa* alkaloids.[4,10,26] Importantly, speciociliatine is the major circulating alkaloid after consumption of kratom in humans, and both speciociliatine and corynantheidine have a higher affinity for hMOR and adrenergic receptors than mitragynine.[10,26] As shown by our results, leaf developmental stage can thus impact kratom pharmacology.

Nuclear DNA Content Estimation Indicates Mitragyna Germplasm Is Tetraploid. The nuclear DNA content of seven cultivars of *M. speciosa*, *Ms* cv 1−7, included in the study was estimated using flow cytometry. DNA content of cultivars ranged from 1.14 to 1.4 pg (Table 2). While the DNA content in *Ms* cv 1 was significantly higher and *Ms* cv 6 was lower than others in this study, these results are in accordance with estimates of *M. speciosa* DNA content of a 2C = 1.45 Gb.[22] However, *Ms* cv. Rifat, authenticated as a tetraploid by chromosome counting ($2n = 4x = 44$; 2C = 1.56 Gb)[21] had higher DNA content than all cultivars reported. All cultivars apart from *Ms* cv 6 are likely tetraploid. *Ms* cv 6 contained a significantly lower DNA content than all other cultivars, suggesting differences in its origin or ploidy. However, such differences must be investigated by chromosome counting, as cytosolic secondary metabolites could interfere with DNA staining and affect quantitative cytometry estimates.

https://doi.org/10.1021/acs.jnatprod.3c00092
J. Nat. Prod. XXXX, XXX, XXX−XXX

Table 1. Targeted Monoterpene Indole or Oxindole Alkaloidal Quantification from Leaf Developmental Stages Represented as w/w % Alkaloid by Dry Mass ± SD[a]

monoterpene indole (or) oxindole alkaloid	juvenile 1 < 4 cm	juvenile 2 < 7 cm	juvenile 3 < 10 cm	medium	mature
mitragynine	0.47 ± 0.15 b	0.95 ± 0.15 ab	1.35 ± 0.06 a	1.42 ± 0.44 a	1.44 ± 0.16 a
speciogynine	0.26 ± 0.08 c	0.44 ± 0.04 abc	0.57 ± 0.02 a	0.53 ± 0.16 ab	0.31 ± 0.06 bc
speciociliatine	1.67 ± 0.32 a	1.7 ± 0.03 a	1.81 ± 0.21 a	1.26 ± 0.34 a	0.45 ± 0.14 b
mitraciliatine	0.23 ± 0.05 a	0.23 ± 0.01 a	0.24 ± 0.02 a	0.16 ± 0.04 a	0.05 ± 0.03 b
7-hydroxymitragynine	0.04 ± 0.02 ab	0.03 ± 0.01 ab	0.05 ± 0.01 a	0.02 ± 0 b	0.01 ± 0 b
paynantheine	0.34 ± 0.06 bc	0.56 ± 0.05 ab	0.8 ± 0.06 a	0.73 ± 0.16 a	0.32 ± 0.04 c
corynantheidine	1.98 ± 0.28 a	1.65 ± 0.08 ab	1.43 ± 0.13 b	0.69 ± 0.22 c	0.11 ± 0.03 d
corynoxine	0.37 ± 0.07 a	0.31 ± 0.03 a	0.3 ± 0.05 a	0.16 ± 0.06 b	0.06 ± 0.01 b
corynoxine-B	0.17 ± 0.04 a	0.14 ± 0 a	0.13 ± 0.03 ab	0.07 ± 0.02 bc	0.03 ± 0.01 c
mitraphylline	below LLOQ	below LLOQ	below LLOQ	below LLOQ	below LLOQ
w/w % crude extract	38.36 ± 1.85 a	32.34 ± 0.96 b	35.5 ± 2 ab	30.64 ± 3.23 bc	26.57 ± 0.49 c

[a]One way ANOVA with Tukey−Kramer HSD multiple comparison tests using JMP. Means (n = 3) sharing the same letter are not statistically different. SD = standard deviation; LLOQ = the lower limit of quantification.

Table 2. DNA Content Estimation of *M. speciosa* Cultivars[a]

M. speciosa	pg of DNA
Ms cv 1	1.4 ± 0.03 a
Ms cv 2*	1.3 ± 0.05 b
Ms cv 3*	1.25 ± 0.02 b
Ms cv 4	1.29 ± 0.04 b
Ms cv 5	1.3 ± 0.03 b
Ms cv 6	1.14 ± 0.08 c
Ms cv 7	1.31 ± 0.02 b

[a]Data represent mean (n = 3 ± SD) picograms DNA. Three technical replicates were analyzed for each sample. Means sharing the same letter are not statistically different from each other at $p < 0.05$. *n = 1.

DNA Barcoding and Phylogenetic Analysis of Mitragyna Germplasm Suggest Interspecific Hybridization Events Resulting in Variable Alkaloid Chemistry. DNA barcoding and phylogenetic analyses using *ITS* nucleotide sequences of six *M. speciosa* cultivars, two commercial products, and other mitragyna species, including *M. parvifolia* and *M. hirsuta*, revealed a well-supported distinction creating several subgroups within *M. speciosa* (Figure 3A). *Ms* cv 1 and 2, as well as commercial products 1 and 2, grouped with *M. speciosa* accession (KC737618.1) sequence from the National Center for Biotechnology Information (NCBI). PCR amplification using DNA extracted from *Ms* cv 6 was unsuccessful. Of the remaining cultivars, *Ms* cv 3−5 and 7 grouped with other *Mitragyna* species with corresponding single-nucleotide polymorphisms (SNPs) and allelic variants in the *ITS* region correlating with other species (Figure 3B). For example, SNPs at positions 42 and 101 in *Ms* cv 3 correspond to *M. hirsuta* and *M. parvifolia*, respectively, suggesting interspecific hybridization (Figure 3B), as those regions distinguish *M. speciosa* from other mitragyna species.[24] Similarly, a single base pair deletion in *M. hirsuta* is present in *Ms* cv 4 and reflected as a frameshift in *Ms* cv 3, 5, and 7, alongside the *M. speciosa* allele, thus yielding heterozygous regions (Figure 3B). These analyses provide evidence that heterozygosity or allelic variation in the *ITS* barcode is associated with low mitragynine content, and the polymorphisms in such cultivars are identical to alleles in other species of mitragyna.[24] Thus, high mitragynine-producing *Ms* cv 1 and 2 were homozygous at *ITS* and may be true to type cultivars, while *Ms* cultivars 3−7 may be hybrid individuals, where the presence of alleles from other species has affected mitragynine content and overall alkaloid profiles. This clearly suggests interspecific hybridization events responsible for the presence of multiple alleles in low mitragynine cultivars, evidenced by the additive effect of *ITS* regions from parents with diverging genomic sequences. In addition to genotypic differences, morphological differences are observable between cultivars. Although the recognizable characteristics of Rubiaceae are present in all cultivars, including opposite, entire evergreen leaves with connation of stipules (Figure 3C, Figure S1), they all differ in leaf morphology (Figure 3D). Interestingly, *Ms* cv 1 and 2 with narrow and elongated leaf shape corresponded to high mitragynine, while rounded leaf cultivars in our germplasm had low or negligible amounts of mitragynine. However, leaf shape alone is insufficient for identification of *M. speciosa* and the corresponding assumption of mitragynine content. Misidentification of mitragyna species is highly likely when contexts of geographical distribution and flower morphology are unavailable, as plant characteristics of the Asian mitragyna species (*M. diversifolia*, *M. hirsuta*, *M. rotundifolia*, and *M. speciosa*) often overlap.[27] However, it is possible to distinguish *M. speciosa* from other mitragyna species using the *ITS* barcoding region.[24]

Characterization of Alkaloids from *M. speciosa* Germplasm Identified Genotype-Dependent Alkaloid Composition and Content Leading to Altered Chemotypes. Quantities of targeted alkaloids (Scheme 1) from *Ms* cv1−7 and products 1 and 2 were determined and illustrated as groups of similar chemical phenotypes (chemotypes) based on the predominant leaf alkaloid (Figure 4, Table S2). Mitragynine was the major alkaloid accumulating in commercial products 1 and 2, as well as *Ms* cv 1 and 2, as expected of *M. speciosa*. Speciociliatine was the second most abundant alkaloid in this group, followed by paynantheine and speciogynine (Figure 4A). Mitraciliatine is the dominant alkaloid in *Ms* cv 3, 4, and 7 (Figure 4B) and speciogynine in *Ms* cv 5 and 6 (Figure 4C). The preferential accumulation of mitraciliatine or speciogynine in potential-hybrid cultivars, which are typically minor alkaloids of *M. speciosa*, further supports the distinction in cultivars. Speciogynine, which is a C-20 epimer of mitragynine (Scheme 1), is not an hMOR agonist like mitragynine, but demonstrated high binding affinity to serotonergic receptors,[5] while mitraciliatine, a diastereomer of mitragynine (Scheme 1), is a partial hMOR agonist similar to mitragynine.[5] These examples indicate the significance of stereochemistry in dictating the pharmaco-

https://doi.org/10.1021/acs.jnatprod.3c00092
J. Nat. Prod. XXXX, XXX, XXX−XXX

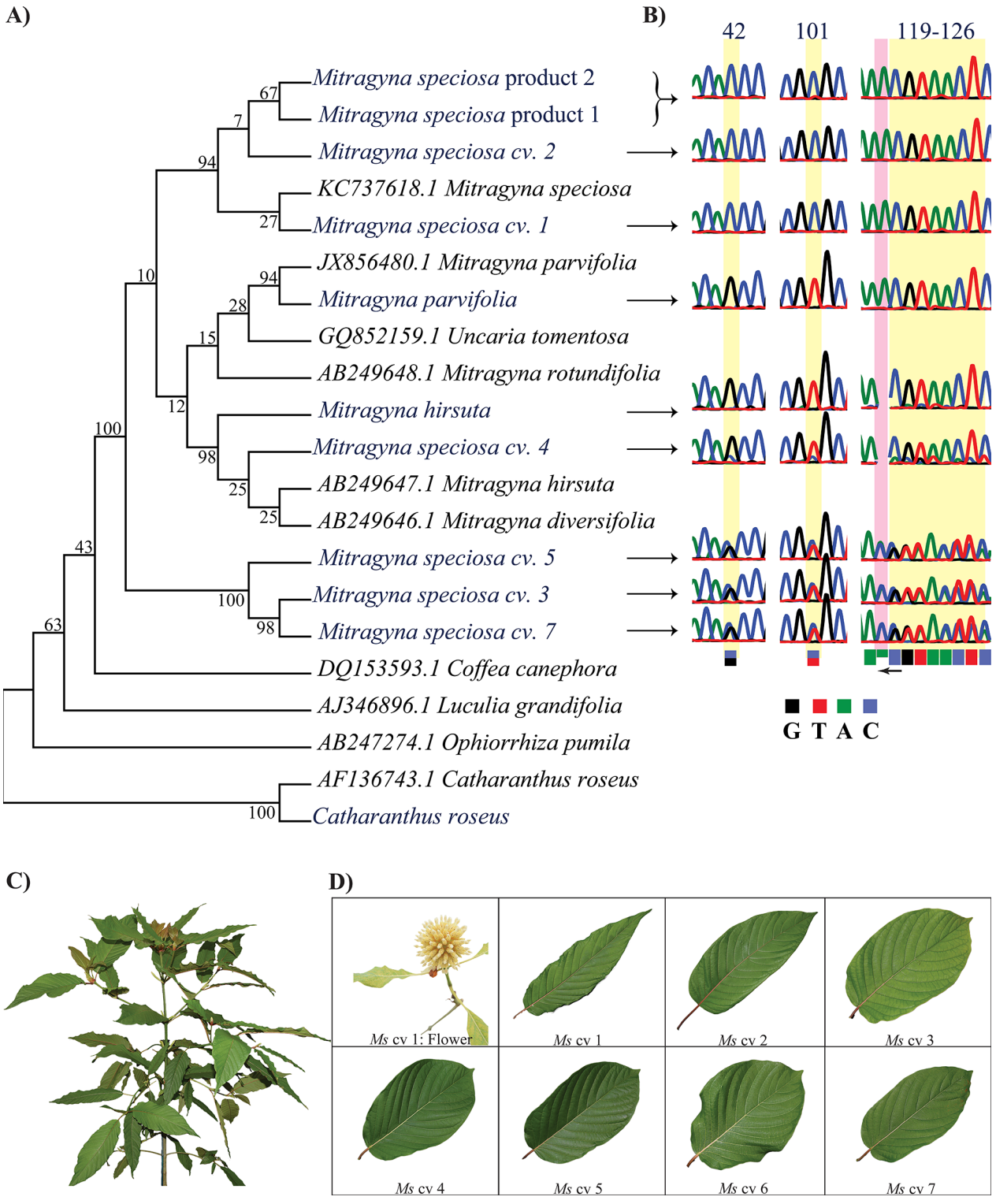

Figure 3. DNA barcoding and phylogenetic analysis of mitragyna cultivars reveal hybridization events. (A) Phylogenetic tree comprising *ITS1* and *ITS2* sequences from fresh tissue (blue) or retrieved from NCBI (black) for several mitragyna cultivars and products used in this study, other mitragyna species, and MIA-producing species. While most *M. speciosa* samples grouped together, well-supported distinction between cultivars created subgroups within *M. speciosa*. (B) Polymorphisms in *ITS* sequences including heterozygosity (highlighted in yellow) in *Ms* cv 3−7, deletion (pink) in *Ms* cv 4, and frameshift in *Ms* cv 3−7, implying the presence of parental genomes with diverging genotypes. (C) *Ms* cv 1 cutting showing typical morphological characteristics of Rubiaceae including opposite entire leaves with connation of stipules. (D) Flowers are terminal heads with creamy or yellow flowers in ball-shaped clusters. Mature leaf morphology of each cultivar in this study with varying leaf shape with *Ms* cv 1 and 2 having expected ovate-accumate shape and redder than *Ms* cv 3−7, which exhibit oblong leaf shapes and midrib coloration ranging from green to red.

https://doi.org/10.1021/acs.jnatprod.3c00092
J. Nat. Prod. XXXX, XXX, XXX−XXX

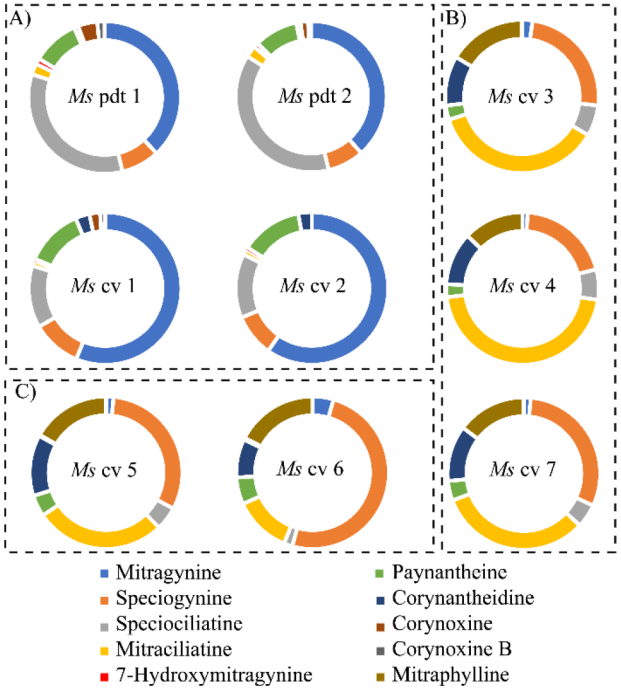

Figure 4. Alkaloid composition of greenhouse-grown *M. speciosa* germplasm. Doughnut diagram represents the relative quantities of alkaloids in cultivars and products of *M. speciosa* based on percentage weight by weight and are grouped by major alkaloid. (A) Mitragynine-dominant cultivars of *M. speciosa*. (B) Mitraciliatine-dominant cultivars of *M. speciosa*. (C) Speciogynine-dominant cultivars of *M. speciosa*.

logical activities of kratom alkaloids and further signifying the importance of polymorphisms in the *ITS* barcode region which correlate to varying alkaloid profiles. *Ms* cv 3−7 were also characterized by the presence of the oxindole alkaloid mitraphylline, which is a predominant alkaloid in cat's claw, *Uncaria*, species[16] in addition to several other mitragyna species, including *M. parvifolia*, *M. hirsuta*, and *M. rotundifolia*, but not *M. speciosa*.[1] This composition held true in both mature and juvenile tissue (Table S2). This further supports the possibility of interspecific hybridization events affecting the alkaloid profiles.

In conjunction with our results, a previous study also reported *M. speciosa* cv. Rifat with low levels of mitragynine[28] that also grouped with *M. hirsuta*, *M. diversifolia*, and *M. parvifolia*. Hybridization is known to impact plant specialized metabolism, leading to novel or missing metabolites, dysregulation of metabolites (up- or down-regulated), and compartmentalization patterns different from either parent.[29] Notably, 7-HMG was detected in both commercial products and *Ms* cv 1 and 2, but was not detected in low-mitragynine-producing cultivars, *Ms* cv 3−7, in mature or juvenile tissue. Due to a lack of access to germplasm and uncertainty around identity, much focus has been placed on cataloging alkaloid composition and characterizing alkaloids in *M. speciosa* grown under different cultivation conditions.[28,30]

Root Transcriptome Sequencing of High- and Low-Mitragynine Chemotypes of *M. speciosa* Reveal Large-Scale Transcriptomic Differences Supporting Hybridization. While the accumulation of mitragynine has been well established to occur in *M. speciosa* leaves,[31] localization of MIA biosynthesis appears to be complex. Previous transcriptomic work found that upstream MIA biosynthetic pathway genes, including methylerythritol 4-phosphate (MEP) and secoiridoid biosynthetic pathway genes, are preferentially expressed in *M. speciosa* roots.[21] This suggested that early biosynthetic steps may be more active in root tissue. Therefore, to analyze gene expression differences between high- and low-mitragynine chemotypes *Ms* cv 2 and 3 (Figure 5A), RNA-seq was performed using RNA extracted from roots of established *Ms* cv 2 and 3 trees growing in Apopka, Florida. A total of 55,746 transcripts were mapped to the reference genome. Genes with low counts (<5 in 75% of samples) were filtered out, and 38,928 genes remained for analysis. Of these, 6429 genes were down-regulated between *Ms* cv 2 and 3, and 15532 genes were up-regulated (false discovery rate (*fdr*) adjusted $p < 0.05$; Figure S3). In the subsequent Kyoto Encyclopedia of Genes and Genomes (KEGG) orthology enrichment analysis, k10268 (leucine-rich repeats, F box, and F-box-like), k10999 (plant cellulose synthase subfamily, glycosyltransferase 2 family), k08679 (UDP-glucuronate 4-epimerase, RmlD substrate-binding domain), and k08245 (saposin (B) domains of peptidase A1 family) were significantly enriched (*fdr* adjusted $p < 0.05$). In conjunction, of the top 25 significant gene ontology (GO) terms, 11 were involved in cytoskeletal motor activity and associated complexes, four in cell wall biogenesis, two in polysaccharide biosynthesis, and two in mitotic cell cycle processes (Table S3). Nearly 60% of genes were differentially expressed (Figure S3), mostly with GO terms indicating differences in root growth and development between cultivars. As a result, identifying candidates in the MIA pathway responsible for variable chemotypes was challenging.

Allelic variation at the transcript level was observed in multiple genes between the two cultivars (Figure 5B). *Ms* cv 2, with relatively high mitragynine content, expressed a single allele at various loci, whereas *Ms* cv 3 was heterozygous with at least two different alleles expressed at each locus. For example, a single *STR* allele, involved in strictosidine biosynthesis, is expressed in *Ms* cv 2 with base A at location 26082:12,964 and base C at 126082:12,975. On the other hand, *Ms* cv 3 at these loci is represented by G and T as dominant alleles, respectively, while A and C represent minor alleles (Figure 5B). Similarly, the reads mapped to the predicted *SLS* (secologanin synthase) have G allele expressed in 99% of *Ms* cv 2 reads at position 127731:524,041, while A and G are expressed in *Ms* cv 3, with A being the major allele. Similarly, at position 127731:524,042 of *SLS*, the T allele is almost uniquely expressed in *Ms* cv 2, but G and T are expressed in *Ms* cv 3, with preferential expression of G (Figure 5B). These findings support our hypothesis that hybridization leading to changes in allelic dosage has impacted the alkaloid composition in *M. speciosa*.

The complexity and compartmentalization of pharmaceutical alkaloids biosynthesis have been noted and are well-studied in several medicinal plant species such as *Catharanthus roseus* (vinblastine), *Atropa belladonna* (hyoscyamine, scopolamine, atropine), and *Papaver somniferum* (morphine).[32] The facts that (i) none of the major alkaloids found in *M. speciosa* leaves are detected in roots, while the upstream biosynthetic genes are preferentially expressed in roots, and (ii) juvenile leaves accumulate significantly high amounts of the mitragynine precursor corynantheidine, which reduces with leaf development with increasing mitragynine until maturity, suggest that there is selective transport and developmental regulation of the *M. speciosa* MIAs. No transporters have yet been identified between aerial and below-ground tissues in *M. speciosa*.

https://doi.org/10.1021/acs.jnatprod.3c00092
J. Nat. Prod. XXXX, XXX, XXX−XXX

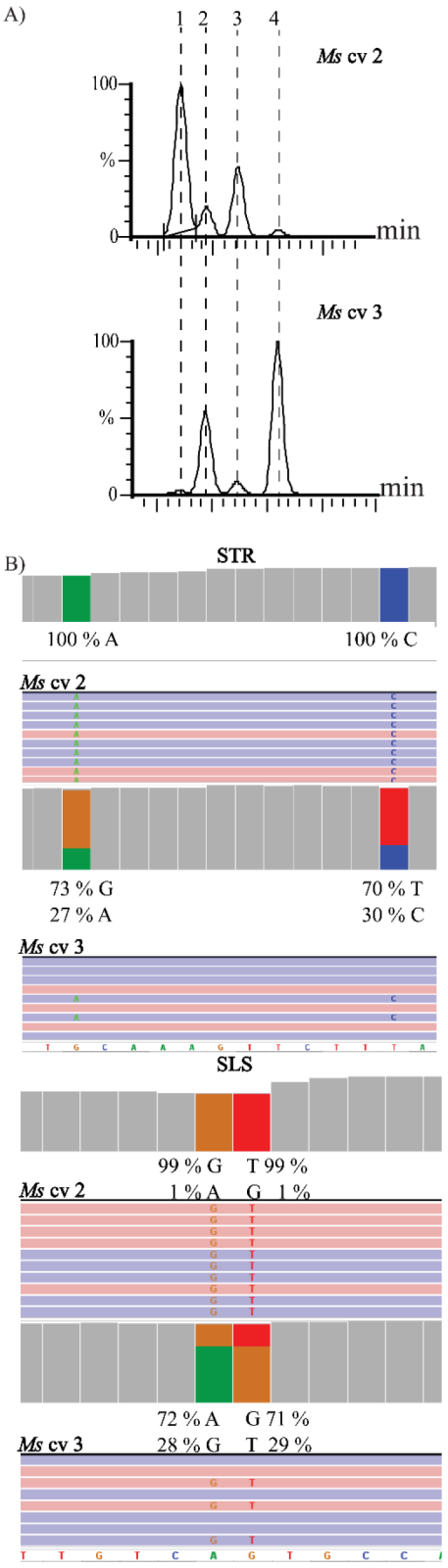

Figure 5. Correlating MIA profiles of high- and low-mitragynine cultivars of *M. speciosa* and their root RNA-seq data. (A) Chromatograms of selected alkaloids (1) mitragynine, (2) speciogynine, (3) speciociliatine, and (4) mitraciliatine showing contrasting chemical phenotypes in *M. speciosa* cultivars 2 and 3. (B) Allelic variant analysis in integrative genome viewer (IGV) comparing single-nucleotide variants (SNVs) identified in *M. speciosa* cv. 2 (top) and 3 (bottom) in the genes strictosidine synthase (*STR*; g51324.t1) and secologanin synthase (*SLS*; g513.1).

Interestingly, a homologue of a nitrate/peptide family (NPF) transporter identified in *C. roseus* as a vacuolar strictosidine transporter was found to have similar expression in roots and juvenile leaves.[21] This suggests that MIA precursors and end products may be separated by intercompartmental trafficking of intermediates. As shown in Figure 1, no mitragynine is formed in the roots, while corynantheidine and stereoisomers of mitragynine, mitraciliatine, and speciociliatine are present in root tissue. Single-cell transcriptome and metabolome of leaf and root tissues may prove useful in deciphering the transport mechanisms.

CONCLUSIONS

M. speciosa germplasm has been characterized based on the predominant alkaloid detected, and the chemotype of an individual cultivar has been correlated with DNA barcoding and phylogenetic analyses. This study demonstrated that the chemical phenotype of *M. speciosa* may be predicted based on DNA barcoding and expression patterns in alleles of MIA pathway homologues. Comparative genomic approaches, including whole genome sequencing and detecting genome-wide polymorphisms in various cultivars, will help in the identification of genomic regions that affect alkaloid metabolism. These genomic regions may be leveraged for developing molecular markers to aid in chemical phenotyping. Such a molecular tool would be invaluable in the quality control and regulation of marketed *M. speciosa* products and further aid in marker-assisted breeding and cultivation of *M. speciosa* varieties with desired alkaloidal composition.

EXPERIMENTAL SECTION

Plant Material and Growth Conditions. *Mitragyna speciosa* cultivars were acquired from Dr. Pearson's study[30] and private plant producers, and details of cultivar names as received have been provided (Table S4). All the cultivars used in the study were received as cuttings and were grown in PRO-MIX BX (Premier Tech Horticulture, Quakertown, PA, USA) in a greenhouse under a light intensity of ∼500−600 μmol m^{-2} s^{-1} and an average temperature of 24 °C. Light measurements were taken with a Weston 756 illumination meter, and night interruption of 4.5 μmol·m^{-2}·s^{-1} for 4 h was implemented that showed improvement in the growth of plants during short days from October to March.[33] Propagation of material for developmental profiling experiments was done by stem cuttings. Stems of plant propagules were dipped into Dip'N Grow rooting solution (Clackamas, OR, USA) at 5× dilution as per manufacturer recommendations and were placed in a mixture of 50% perlite and 50% vermiculite at ∼500 μmol m^{-2} s^{-1} in a mist house set to 5 s of misting every 5 min with high relative humidity (>50%). Once roots were well established (4−6 weeks), propagules were transplanted into 4 in. pots containing PRO-MIX BX and moved to a greenhouse maintained under the above-mentioned conditions. Two months after transplanting, plants are transferred into larger 3-gallon containers. Fertilizer was applied by fertigation (100 ppm: Peters Professional 20−10−20), and plants were irrigated daily.

DNA Barcoding of *Mitragyna* Germplasm. Genomic DNA was extracted from young, immature leaves of *M. speciosa* that were flash-frozen and ground in liquid nitrogen into a fine powder or commercial products available as dried powders, using a modified hexadecyltrimethylammonium bromide (CTAB) protocol[34] optimized for *M. speciosa*. To each sample was added 500 μL of extraction buffer (0.35 M sorbitol, 0.1 M Tris-HCl, 5 mM EDTA, pH 7.5; preheated to 65 °C) containing 0.3% β-mercaptoethanol, 1% w/v polyvinylpyrrolidone (PVP) 40,000, and 300 μL of nuclear lysis buffer (0.2 M Tris-HCl, 0.05 M EDTA, 2 M NaCl, 2% w/v CTAB). Samples were incubated at 65 °C for 1 h, with gentle inversion every 20 min. After cooling to room temperature, 800 μL of chloroform−isoamyl

https://doi.org/10.1021/acs.jnatprod.3c00092
J. Nat. Prod. XXXX, XXX, XXX−XXX

alcohol (24:1) was added and mixed by inversion. Samples were centrifuged at 13,000 rpm for 15 min at room temperature, the aqueous layer (top layer) was collected, and the extraction step was repeated until the aqueous layer was clear. To the final recovered aqueous solution, 0.5 volume of 6 M NaCl and 0.1 volume of 3 M KCl were added and mixed well. DNA was precipitated with 1 volume of ice-cold isopropanol, pelleted, and washed with 1 mL of 70% cold ethanol. The pellet was dried and dissolved in nuclease-free molecular-grade deionized water.

The *ITS* gene was amplified from genomic DNA by Phusion high-fidelity DNA polymerase (New England BioLabs, Ipswich, MA, USA) with the mixed base oligos ITS-u1 (GGAAGKARAAGTCGTAACAAGG) and ITS-u4 (RGTTTCTTTTCCTCCGCTTA).[35] DNA extracted from *M. speciosa* cv 6 yielded no amplification and could not be included in barcoding and phylogenetic analyses. The PCR products were purified using Wizard SV gel and PCR clean-up system (Promega Madison, WI, USA), and 60−100 ng of purified PCR product was submitted for Sanger sequencing to GeneWiz (https://www.genewiz.com) per submission guidelines. Resulting sequences were analyzed by Sequencher version 5.4.6 (Gene Codes Corp., Ann Arbor, MI, USA) and GEAR genomics application PEARL (https://www.gear-genomics.com).

Molecular Phylogenetic Analysis. *ITS* nucleotide sequences from our germplasm, along with sequences available in the NCBI nucleotide database, were aligned using MUSCLE (default alignment parameters: gap penalties: −400 open; −0 extend; cluster method UPGMA) in MEGA11 (version 11.0.13). A maximum likelihood phylogenetic tree (Tamura 3-parameter with a discrete gamma distribution; bootstrapped 1000 times) was generated using multiple sequence alignments using MEGA11.

Determination of Nuclear DNA Content by Flow Cytometry. The nuclear DNA content of mitragyna cultivars was determined using a Sysmex CyFlow flow cytometer (BD Biosciences, San Jose, CA, USA) using tomato (*Solanum lycopersicum* L. 'Stupické polní rané') as an internal standard.[36] We utilized CyStain PI Absolute P kit (Sysmex, Lincolnshire, IL, USA), which included nuclei extraction buffer, staining buffer, propidium iodide, and RNaseA. RNaseA stock solution was prepared by adding 1.5 mL of water (nuclease-free, molecular biology grade, ultrapure, Thermo Scientific) to five RNaseA tubes per the manufacturer's instruction. The staining solution was prepared freshly on the day of analysis by adding 120 μL of propidium iodide and 60 μL of RNaseA stock solution to 20 mL of staining buffer. A 30 mg amount of young leaves of mitragyna cultivars and tomato internal standard were finely chopped into 500 μL of nuclei extraction buffer in a Petri dish. The homogenate was incubated for 90 s, then filtered through a nylon mesh (30 μm CellTrics filters, Sysmex) into a sample tube provided. A 2 mL amount of staining solution was added to the filtered homogenate. Three biological replicates of each cultivar and a plant each for *Ms* cv 2 and cv 3 and three technical replicates of each sample were analyzed. Nuclear DNA content of each sample was calculated as (nuclear DNA content of internal standard × mean fluorescence value of sample)/mean fluorescence value of the internal standard.

RNA Sequencing and Analysis. High-quality RNA was isolated from three biological replicates of *Ms* cv 2 and 3 root tissue using the protocol as described.[21] RNA integrity was assessed using the RNA 6000 Nano kit (Bioanalyzer 2100). Library construction and sequencing were performed at UF ICBR Gene Expression Core and ICBR NextGen Sequencing, respectively. Briefly, reagents provided in the NEBNext Poly(A) mRNA magnetic isolation module (New England Biolabs, catalog #E7490) and the NEBNext Ultra II Directional RNA library prep kit (New England Biolabs, catalog #E7760) were used according to the manufacturer's user guide for library preparation, fragmentation, adaptor ligation, and library amplification. Samples were pooled equimolarly and sequenced simultaneously on an Illumina NovaSeq 6000 for 2 × 150 cycles. Read quality was evaluated using FastQC (v 0.11.9). Sequences were trimmed for quality and adapters and filtered using Trimmomatic v 0.36. Only high-quality (QC > 30) and paired reads were used to align to the available kratom reference genome using HISAT2 (v 2.2.1). Transcript abundance was estimated using htseq-count (v 2.0.0). Replicate homogeneity was checked using a multidimensional scaling analysis with the R package edgeR (v3.36.0). The expression of transcripts across samples was normalized using TMM normalization to control for variations in library size. Sample groups were compared for differential expression using edgeR. Genes with a log-2-fold change of ±1 and *fdr* adjusted (<0.05) *p*-value < 0.05 were marked as differentially expressed genes (DEGs). Gene annotations and predicted coding sequences were downloaded from the Medicinal Plant Genomic Resource (mpgr.uga.edu). EggNOG-mapper[37] was used to generate GO and KEGG terms. Enrichment analysis was carried out using clusterProfiler (v 4.6.0).[38] The Integrative Genome Viewer (IGV) was used for variant review of several MIA pathway genes of interest in the contrasting cultivars with a single nucleotide variants (SNV) calling threshold of 25%.

Extraction of Targeted Alkaloids from *Mitragyna* Tissues. Leaves, stems, roots, and stipules from three biological replicates of *M. speciosa* cv 1 were flash frozen, ground to a fine powder in liquid nitrogen, and stored at −80 °C until used. Leaf developmental stages were defined based on size and position: jv1 (<4 cm; juvenile 1), jv2 (<7 cm), jv3 (<10 cm), medium (>10 cm), and mature. Mature leaves were collected from the main stem, two nodes below the apical meristem. For characterization of germplasm from cultivars 2−7, jv2 or jv3 leaves and mature leaves from an individual for each cultivar were flash frozen and processed as described above. Prior to alkaloid extractions, all ground tissues were lyophilized in a benchtop freeze-dryer (FreeZone, Labconco, Kansas City, MO, USA) for 24 h at ∼0.5 mbar and −90 °C to obtain dry weights. A 50 mg amount of lyophilized tissue was extracted with 1 mL of 100% ethanol and sonicated for 90 min. The solution was centrifuged at 4000 rpm for 5 min, after which the extracts were removed from insoluble material by pipetting or using a syringe filter (0.2 μm pore; Sigma-Aldrich). Extraction was repeated three times per sample to ensure complete extraction of alkaloids as optimized previously.[39] The filtrates from all three extractions were combined, and the solvent was evaporated using a nitrogen line evaporator at 37 °C. The recovered extracts were then lyophilized to complete dryness for 24 h at ∼0.5 mbar and −90 °C. The dried fractions were accurately weighed for total crude extract determination and dissolved in methanol for analysis.

Identification and Quantification of Alkaloids by UPLC-MS/MS. Identification and quantification of targeted alkaloids were performed as previously described[39] using a Waters Acquity Class I ultraperformance liquid-chromatography (UPLC) coupled with a XevoTQ-S Micro triple quadrupole mass spectrometer (Milford, MA, USA) for the simultaneous quantification of 10 indole and oxindole alkaloids (Scheme 1). The standards of mitragynine, speciogynine, speciociliatine, mitraciliatine, 7-HMG, corynantheidine, paynantheine, mitraphylline, corynoxine, and corynoxine-B were isolated and purified from dried *M. speciosa* leaves previously.[39] Briefly, alkaloids were subjected to proton and carbon nuclear magnetic resonance (^{1}H NMR, ^{13}C NMR), high-performance liquid chromatography−photometric diode array (HPLC−PDA), and UPLC-quadrupole time-of-flight (QTOF) to determine purity and subsequently used for quantitation in the study.[39] A method reported by Sharma et al.[39] was partially modified to reduce the total analysis time per sample. Samples were processed and diluted as previously described,[39] and 2 μL of crude alkaloid extract in methanol−water (50:50, %v/v) for each sample was injected for chromatographic separation on a Waters Acquity BEH C18 column (1.7 μm, 2.1 × 100 mm) using an aqueous ammonium acetate buffer (2.5 mM, pH 3.5) (A) and acetonitrile (B) as mobile phase flowing at 0.35 mL min^{-1} with the following gradient: A, 80% for 1 min, linear decrease to 77% by 6 min, followed by linear decrease to 10% in 2 min and maintained for 0.5 min. The column was reequilibrated to initial condition (80%) for 0.7 min. Data acquisition and analysis were performed by MassLynx XS version 4.1. Alkaloid quantities are reported as mass percent analyte per dried tissue extracted.

Statistical Analysis. One-way ANOVA was used to compare mean alkaloidal content among different tissue types and developmental stages, and *posthoc* mean comparisons were tested by

https://doi.org/10.1021/acs.jnatprod.3c00092
J. Nat. Prod. XXXX, XXX, XXX−XXX

Tukey−Kramer honest significant difference (HSD) multiple comparison tests using JMP Pro 15.0.0 (SAS Institute, Cary, NC). Alkaloids that were undetectable due to limits of quantification were treated as zero for statistical analysis.

■ ASSOCIATED CONTENT

Supporting Information

The Supporting Information is available free of charge at https://pubs.acs.org/doi/10.1021/acs.jnatprod.3c00092.

Supplemental tables (Tables S1−S5) and supplemental figures (Figures S1−S3) (PDF)

Accession Codes

M. speciosa, *M. parvifolia*, and *M. hirsuta ITS* sequences have been submitted to NCBI GenBank databases under the accession numbers OQ244095−OQ244104 (Table S5). Raw sequence reads for transcriptomic analysis are available through the NCBI Sequence Read Archive under BioProject ID PRJNA923664. All other data are available by request to the corresponding author.

■ AUTHOR INFORMATION

Corresponding Author

Satya Swathi Nadakuduti − *Plant Molecular and Cell Biology Program, University of Florida, Gainesville, Florida 32611, United States; Department of Environmental Horticulture, University of Florida, Gainesville, Florida 32606, United States;* orcid.org/0000-0002-0831-3760; Email: s.nadakuduti@ufl.edu

Authors

Larissa C. Laforest − *Plant Molecular and Cell Biology Program, University of Florida, Gainesville, Florida 32611, United States*

Michelle A. Kuntz − *Department of Pharmaceutics, College of Pharmacy, University of Florida, Gainesville, Florida 32611, United States*

Siva Rama Raju Kanumuri − *Department of Pharmaceutics, College of Pharmacy, University of Florida, Gainesville, Florida 32611, United States;* orcid.org/0000-0002-6087-6587

Sushobhan Mukhopadhyay − *Department of Medicinal Chemistry, College of Pharmacy, University of Florida, Gainesville, Florida 32611, United States*

Abhisheak Sharma − *Department of Pharmaceutics, College of Pharmacy, University of Florida, Gainesville, Florida 32611, United States;* orcid.org/0000-0003-0553-4039

Sarah E. O'Connor − *Department of Natural Product Biosynthesis, Max Planck Institute for Chemical Ecology, 07745 Jena, Germany;* orcid.org/0000-0003-0356-6213

Christopher R. McCurdy − *Department of Medicinal Chemistry, College of Pharmacy, University of Florida, Gainesville, Florida 32611, United States;* orcid.org/0000-0001-8695-2915

Complete contact information is available at: https://pubs.acs.org/10.1021/acs.jnatprod.3c00092

Author Contributions

The manuscript was written through contributions of all authors. All authors have given approval to the final version of the manuscript.

Funding

Funding for S.S.N. was provided by the USDA-NIFA Hatch project #006010, a startup fund from the Environmental Horticultural Department and Institute of Food and Agricultural Sciences at the University of Florida. A portion of this study was made possible by NIDA grants DA047855 and DA048353.

Notes

The authors declare no competing financial interest.

■ ACKNOWLEDGMENTS

We would like to thank Dr. Brian Pearson and growers, Apopka, FL, for sharing the cultivars of *M. speciosa* and Mengzi Zhang for providing guidance with propagation of the material. We thank Dr. Robin Buell for valuable discussions on transcriptomic analyses.

■ REFERENCES

(1) Brown, P. N.; Lund, J. A.; Murch, S. J. *J. Ethnopharmacol* **2017**, *202*, 302−325.

(2) Han, C.; Schmitt, J.; Gilliland, K. M. *ACS Chem. Neurosci.* **2020**, *11* (23), 3870−3880.

(3) Flores-Bocanegra, L.; Raja, H. A.; Graf, T. N.; Augustinović, M.; Wallace, E. D.; Hematian, S.; Kellogg, J. J.; Todd, D. A.; Cech, N. B.; Oberlies, N. H. *J. Nat. Prod* **2020**, *83* (7), 2165−2177.

(4) Kamble, S. H.; Berthold, E. C.; King, T. I.; Raju Kanumuri, S. R.; Popa, R.; Herting, J. R.; León, F.; Sharma, A.; McMahon, L. R.; Avery, B. A.; McCurdy, C. R. *J. Nat. Prod* **2021**, *84* (4), 1104−1112.

(5) Smith, K. E.; Sharma, A.; Grundmann, O.; McCurdy, C. R. *ACS Chem. Neurosci.* **2023**, *14*, 195.

(6) Allen, B.; Feldman, J. M.; Paone, D. Public Health and Police: Building Ethical and Equitable Opioid Responses. *Proc. Natl. Acad. Sci. U.S.A.* **2021**, *118* (45), DOI: 10.1073/pnas.2118235118.

(7) Singh, D.; Narayanan, S.; Vicknasingam, B. *Brain Res. Bull.* **2016**, *126*, 41−46.

(8) Coe, M. A.; Pillitteri, J. L.; Sembower, M. A.; Gerlach, K. K.; Henningfield, J. E. *Drug Alcohol Depend* **2019**, *202*, 24−32.

(9) Sharma, A.; McCurdy, C. R. *Expert Opin Drug Metab Toxicol* **2021**, *17* (3), 255−257.

(10) Obeng, S.; Kamble, S. H.; Reeves, M. E.; Restrepo, L. F.; Patel, A.; Behnke, M.; Chear, N. J. Y.; Ramanathan, S.; Sharma, A.; León, F.; Hiranita, T.; Avery, B. A.; McMahon, L. R.; McCurdy, C. R. *J. Med. Chem.* **2020**, *63* (1), 433−439.

(11) Hemby, S. E.; McIntosh, S.; Leon, F.; Cutler, S. J.; McCurdy, C. R. *Addiction Biology* **2019**, *24* (5), 874−885.

(12) Yue, K.; Kopajtic, T. A.; Katz, J. L. *Psychopharmacology (Berl)* **2018**, *235* (10), 2823−2829.

(13) Chear, N. J. Y.; León, F.; Sharma, A.; Kanumuri, S. R. R.; Zwolinski, G.; Abboud, K. A.; Singh, D.; Restrepo, L. F.; Patel, A.; Hiranita, T.; Ramanathan, S.; Hampson, A. J.; McMahon, L. R.; McCurdy, C. R. *J. Nat. Prod* **2021**, *84* (4), 1034−1043.

(14) Hiranita, T.; Obeng, S.; Sharma, A.; Wilkerson, J. L.; McCurdy, C. R.; McMahon, L. R. In Vitro and in Vivo Pharmacology of Kratom. In *Advances in Pharmacology*; Li, J.-X., Ed.; Academic Press, 2022; Vol. 93, pp 35−76; DOI: 10.1016/bs.apha.2021.10.001.

(15) León, F.; Habib, E.; Adkins, J. E.; Furr, E. B.; Mccurdy, C. R.; Cutler, S. J. *Nat. Prod Commun.* **2009**, *4* (7), 907−910.

(16) Montserrat-De La Paz, S.; de La Puerta, R.; Fernandez-Arche, A.; Quilez, A. M.; Muriana, F. J. G.; Garcia-Gimenez, M. D.; Bermudez, B. *J. Ethnopharmacol* **2015**, *170*, 128−135.

(17) O'Connor, S. E.; Maresh, J. J. *Nat. Prod Rep* **2006**, *23* (4), 532−547.

(18) Stander, E. A.; Cuello, C.; Birer-Williams, C.; Kulagina, N.; Jansen, H. J.; Carqueijeiro, I.; Méteignier, L.-V.; Vergès, V.; Oudin, A.; Papon, N.; Dirks, R. P.; Jensen, M. K.; O'Connor, S. E.; Dugé de Bernonville, T.; Besseau, S.; Courdavault, V. The Vinca Minor Genome Highlights Conserved Evolutionary Traits in Monoterpene

Indole Alkaloid Synthesis. *G3 Genes|Genomes|Genetics* **2022**, *12* (12), DOI: 10.1093/g3journal/jkac268.
(19) Caputi, L.; Franke, J.; Farrow, S. C.; Chung, K.; Payne, R. M. E.; Nguyen, T.-D.; Dang, T.-T. T.; Carqueijeiro, I. S. T.; Koudounas, K.; de Bernonville, T. D.; Ameyaw, B.; Jones, D. M.; Curcino Vieira, I. J.; Courdavault, V.; O'Connor, S. E. *Science* **2018**, *360* (6394), 1235−1238.
(20) Chung, K.; O'Connor, S. E. Biosynthesis of Vinblastine. In *Comprehensive Natural Products III*; Elsevier Ltd., 2020; Vol. *2*, pp 642−685; DOI: 10.1016/b978-0-12-409547-2.14618-9.
(21) Brose, J.; Lau, K. H.; Dang, T. T. T.; Hamilton, J. P.; Martins, L. D. V.; Hamberger, B.; Hamberger, B.; Jiang, J.; O'Connor, S. E.; Buell, C. R. The Mitragyna Speciosa (Kratom) Genome: A Resource for Data-Mining Potent Pharmaceuticals That Impact Human Health. *G3* **2021**, *11* (4), DOI: 10.1093/g3journal/jkab058.
(22) Pootakham, W.; Yoocha, T.; Jomchai, N.; Kongkachana, W.; Naktang, C.; Sonthirod, C.; Chowpongpang, S.; Aumpuchin, P.; Tangphatsornruang, S. *Biology (Basel)* **2022**, *11* (10), 1492.
(23) Schotte, C.; Jiang, Y.; Grzech, D.; Dang, T.-T. T.; Laforest, L.; León, F.; Mottinelli, M.; Nadakuduti, S. S.; McCurdy, C. R.; O'Connor, S. E. Directed Biosynthesis of Mitragynine Stereoisomers. *J. Am. Chem. Soc.* **2023**, DOI: 10.1021/jacs.2c13644.
(24) Sukrong, S.; Zhu, S.; Ruangrungsi, N.; Phadungcharoen, T.; Palanuvej, C.; Komatsu, K. *Biol. Pharm. Bull.* **2007**, *30* (7), 1284−1288.
(25) Kitajima, M.; Nakayama, T.; Kogure, N.; Wongseripipatana, S.; Takayama, H. *J. Nat. Med.* **2007**, *61* (2), 192−195.
(26) Kamble, S. H.; Berthold, E. C.; Kanumuri, S. R. R.; King, T. I.; Kuntz, M. A.; León, F.; Mottinelli, M.; McMahon, L. R.; McCurdy, C. R.; Sharma, A. *AAPS Journal* **2022**, *24* (5), 1−16.
(27) Ngernsaengsaruay, C.; Leksungnoen, N.; Boonthasak, W.; Uthairatsamee, S.; Racharak, P.; Leetanasakskul, K.; Pongamorn, P.; Saengbuapuean, A. *Thai Forest Bulletin (Botany)* **2022**, *50*, 20−39.
(28) Todd, D. A.; Kellogg, J. J.; Wallace, E. D.; Khin, M.; Flores-Bocanegra, L.; Tanna, R. S.; Mcintosh, S.; Raja, H. A.; Graf, T. N.; Hemby, S. E.; Paine, M. F.; Oberlies, N. H.; Cech, N. B. Chemical Composition and Biological Effects of Kratom (Mitragyna Speciosa): In Vitro Studies with Implications for Efficacy and Drug Interactions. *Sci. Rep.* **2020**, *10*, DOI: 10.1038/s41598-020-76119-w.
(29) Cheng, D.; Vrieling, K.; Klinkhamer, P. G. L. *Phytochemistry Reviews* **2011**, *10* (1), 107−117.
(30) Zhang, M.; Sharma, A.; León, F.; Avery, B.; Kjelgren, R.; McCurdy, C. R.; Pearson, B. J. *PLoS One* **2022**, *17* (4), e0259326.
(31) Phongprueksapattana, S.; Putalun, W.; Keawpradub, N.; Wungsintaweekul, J. *Z. Naturforsch C J. Biosci* **2008**, *63* (9−10), 691−698.
(32) Watkins, J. L.; Facchini, P. J. *Curr. Opin Plant Biol.* **2022**, *66*, 102186.
(33) Flores, S.; Retana-Cordero, M.; Fisher, P. R.; Freyre, R.; Gómez, C. *HortScience* **2021**, *141* (2), 1476−1485.
(34) Porebski, S.; Bailey, L. G.; Baum, B. R. *Plant Mol. Biol. Report* **1997**, *15* (1), 8−15.
(35) Cheng, T.; Xu, C.; Lei, L.; Li, C.; Zhang, Y.; Zhou, S. *Mol. Ecol Resour* **2016**, *16* (1), 138−149.
(36) Doležel, J.; Greilhuber, J.; Suda, J. *Nat. Protoc* **2007**, *2*, 2233−2244.
(37) Cantalapiedra, C. P.; Hernández-Plaza, A.; Letunic, I.; Bork, P.; Huerta-Cepas, J. *Mol. Biol. Evol.* **2021**, *38* (12), 5825−5829.
(38) Wu, T.; Hu, E.; Xu, S.; Chen, M.; Guo, P.; Dai, Z.; Feng, T.; Zhou, L.; Tang, W.; Zhan, L.; Fu, X.; Liu, S.; Bo, X.; Yu, G. ClusterProfiler 4.0: A Universal Enrichment Tool for Interpreting Omics Data. *Innovation* **2021**, *2* (3), DOI: 10.1016/j.xinn.2021.100141.
(39) Sharma, A.; Kamble, S. H.; León, F.; Chear, N. J. Y.; King, T. I.; Berthold, E. C.; Ramanathan, S.; McCurdy, C. R.; Avery, B. A. *Drug Test Anal* **2019**, *11* (8), 1162−1171.

https://doi.org/10.1021/acs.jnatprod.3c00092
J. Nat. Prod. XXXX, XXX, XXX−XXX